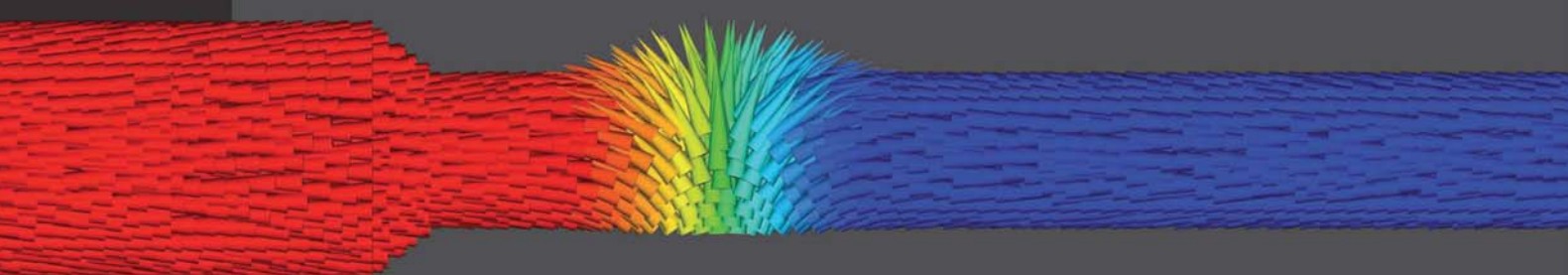


Magnetization Reversal in Cylindrical Nanowires and in Nanowires with Perpendicular Magnetic Anisotropy

Judith Kimling



Cuvillier Verlag Göttingen
Internationaler wissenschaftlicher Fachverlag



Magnetization Reversal in Cylindrical Nanowires and in Nanowires with Perpendicular Magnetic Anisotropy



Dieses Werk ist copyrightgeschützt und darf in keiner Form vervielfältigt werden noch an Dritte weitergegeben werden.
Es gilt nur für den persönlichen Gebrauch.



MAGNETIZATION REVERSAL
IN CYLINDRICAL NANOWIRES
AND IN
NANOWIRES WITH PERPENDICULAR
MAGNETIC ANISOTROPY

Dissertation
zur Erlangung des Doktorgrades
des Fachbereichs Physik
der Universität Hamburg

vorgelegt von
Judith Valentina Kimling
geb. Moser
aus
Ellwangen

Hamburg
2012



Bibliografische Information der Deutschen Nationalbibliothek

Die Deutsche Nationalbibliothek verzeichnet diese Publikation in der Deutschen Nationalbibliografie; detaillierte bibliografische Daten sind im Internet über <http://dnb.d-nb.de> abrufbar.

1. Aufl. - Göttingen: Cuvillier, 2013
Zugl.: Hamburg, Univ., Diss., 2012

ISBN 978-3-95404-518-1

Gutachter der Dissertation:

PD Dr. Guido Meier
Prof. Dr. Manfred Albrecht

Gutachter der Disputation:

PD Dr. Guido Meier
Prof. Dr. Cornelius Nielsch

Datum der Disputation:

14.12.2012

Vorsitzender des Prüfungsausschusses:

Dr. Stefan Mendach

Vorsitzender des Promotionsausschusses:

Prof. Dr. Peter Hauschildt

Dekan der MIN-Fakultät:

Prof. Dr. Heinrich Graener

© CUVILLIER VERLAG, Göttingen 2013
Nonnenstieg 8, 37075 Göttingen
Telefon: 0551-54724-0
Telefax: 0551-54724-21
www.cuvillier.de

Alle Rechte vorbehalten. Ohne ausdrückliche Genehmigung des Verlages ist es nicht gestattet, das Buch oder Teile daraus auf fotomechanischem Weg (Fotokopie, Mikrokopie) zu vervielfältigen.

Gedruckt auf umweltfreundlichem, säurefreiem Papier aus nachhaltiger Forstwirtschaft.



Dieses Werk ist copyrightgeschützt und darf in keiner Form vervielfältigt werden noch an Dritte weitergegeben werden.
Es gilt nur für den persönlichen Gebrauch.



Dieses Werk ist copyrightgeschützt und darf in keiner Form vervielfältigt werden noch an Dritte weitergegeben werden.
Es gilt nur für den persönlichen Gebrauch.

Abstract

Deposition of magnetic materials in self-organized pores of an alumina membrane provides the unique ability to process large amounts of nanowires with complex shape and uniform properties. For both fundamental research and technological applications it is of interest to understand and control the magnetization reversal and the pinning of magnetic domain walls in so-prepared structures. The present work provides new insights into the magnetic behavior of electrochemically synthesized nanowires by applying established methods such as magnetoresistance measurements and magnetic force microscopy as well as a novel photoemission electron microscopy method developed at the synchrotron light source BESSY II in Berlin, Germany. Recording both the electrons emitted directly from the surface of a nanoobject as well as the ones bounced out of the substrate by the transmitted x rays in the object's shadow, surface and bulk magnetizations can be probed separately. The individual switching of two coaxial nanomagnets, namely an iron oxide tube and an enclosed nickel core, is successfully demonstrated.

Magnetization reversal of individual straight nickel wires with diameters between 40 nm and 350 nm is studied experimentally and by micromagnetic simulations performed with nmag. The results are analyzed by comparison to analytical models. For the preparation of domain walls in electrochemically synthesized nanowires three different methods are explored. While the manipulation with a focused Ga^+ ion beam rather decreases the nucleation field than induces pinning sites, reliable domain-wall preparation is shown in bent wires. A main focus of this work lies on magnetization reversal in cylindrical wires with one or more diameter modulations. It is found that domain walls stop their propagation when approaching a modulation from a thin towards a thicker segment. A model based on magnetic charges is proposed that accounts for the experimentally observed behavior and predicts what is also confirmed by micromagnetic simulations: while the exact shape of a modulation is of minor importance, the force experienced by a domain wall and thereby the pinning potential can be tuned by changing the aspect ratio of a modulation.

The last part of this thesis reports on domain nucleation and pinning of domain walls in flat nanowires with perpendicular magnetic anisotropy patterned by electron-beam lithography, sputter deposition of a Co/Pt multilayer, and lift-off processing. Magnetization reversal was imaged by transmission X-ray microscopy at the Advanced Light Source in Berkeley, CA, USA. It is found that the nucleation field in Co/Pt wires can be tuned and reduced by up to 60 percent by designing triangular-pointed ends. In order to clarify the origin of the reduction of the nucleation field micromagnetic simulations are employed. The effect cannot be explained by the geometry variation alone, but is attributable to a local reduction of the perpendicular anisotropy caused by shadowing of the resist mask during sputter deposition of the multilayer. Related aspects concerning the creation of pinning sites for domain walls are addressed.



Dieses Werk ist copyrightgeschützt und darf in keiner Form vervielfältigt werden noch an Dritte weitergegeben werden.
Es gilt nur für den persönlichen Gebrauch.

Zusammenfassung

Die vorliegende Arbeit gewährt neue Einblicke in das magnetische Verhalten elektrochemisch synthetisierter Nanodrähte. Hierfür werden sowohl etablierte Methoden wie Magnetowiderstandsmessungen und magnetische Rasterkraftmikroskopie als auch ein im Rahmen dieser Arbeit neu entwickeltes Verfahren zur Untersuchung komplexer magnetischer Strukturen angewendet. Letzteres nutzt die Strahlenquelle des Berliner Elektronen Synchrotrons BESSY II und basiert auf der konventionell nur oberflächensensitiven Photoemissions-Elektronenmikroskopie. Es werden sowohl die Photoelektronen detektiert, die direkt aus der Oberfläche eines Nanoobjekts emittiert werden, als auch diejenigen, die von den durchdringenden Röntgenstrahlen im Schatten des Objekts aus dem Substrat ausgeschlagen werden. Dadurch gelingt es, Bilder der gesamten Magnetisierung, also von der Oberfläche und aus dem Inneren der Nanostruktur, aufzunehmen. Das Potential der Methode wird durch die Untersuchung von Eisenoxidröhren, die einen Nickel-Kern enthalten, demonstriert. Dabei lässt sich individuelles Schalten der beiden koaxialen Nanomagnete nachweisen.

Darüberhinaus beschäftigt sich die Arbeit sowohl experimentell als auch in mikromagnetischen Simulationen mit den Ummagnetisierungsvorgängen einzelner gerader Nickel-Nanodrähte mit Durchmessern zwischen 40 nm und 350 nm. Die Ergebnisse werden unter anderem anhand analytischer Modelle interpretiert. Für die Präparation von Domänenwänden in elektrochemisch synthetisierten Nanodrähten werden drei verschiedene Methoden erprobt. Während die Manipulation mit einem fokussierten Gallium-Ionenstrahl eher das Nukleationsfeld um circa 10 Prozent verringert, als Pinningzentren zu kreieren, gelingt es durch das Anlegen externer Magnetfelder zuverlässige Domänenwandpräparation in geknickten Drähten zu demonstrieren. Ein Schwerpunkt liegt auf der Untersuchung zylindrischer Drähte mit einer oder mehreren Durchmessermodulationen. Es wird gezeigt, dass Domänenwände stoppen, wenn sie von einem dünnen Segment aus auf die Modulation zu einem dickeren Segment hin zulaufen. Zur Erklärung des experimentell beobachteten Verhaltens wird ein Modell aufgestellt, welches auf magnetischen Ladungen beruht und zudem mikromagnetische Simulationen bestätigt: während die genaue Form einer Modulation nur eine untergeordnete Rolle spielt, kann die von der Domänenwand erfahrene Kraft durch das Aspektverhältnis der Modulation eingestellt werden.

Der letzte Abschnitt der vorliegenden Arbeit beschäftigt sich mit der Nukleation und dem Pinnen von Domänenwänden in lithographisch herstellten Co/Pt-Multischichtdrähten mit senkrechter Anisotropie. Mittels Transmissions-Röntgenmikroskopie an der Advanced Light Source in Berkeley (USA) wird gezeigt, dass das Feld, bei dem Domänenwände in einen Draht injiziert werden, justiert und um bis zu 60 Prozent reduziert werden kann, indem man Drähte mit spitzen Enden herstellt. Mikromagnetische Simulationen belegen, dass die Verringerung dieses Nukleationsfeldes nicht durch die geometrische Variation allein erklärbar ist, sondern sich auf eine Verminderung der lokalen senkrechten Anisotropie zurückführen lässt. Für letztere wiederum sind präparationsbedingte Abschattungseffekte verantwortlich.



Dieses Werk ist copyrightgeschützt und darf in keiner Form vervielfältigt werden noch an Dritte weitergegeben werden.
Es gilt nur für den persönlichen Gebrauch.



Contents

1	Introduction	1
2	Fundamentals	5
2.1	Ferromagnetism	5
2.1.1	Origin of ferromagnetism	5
2.1.2	Magnetic anisotropy	8
2.1.3	Vector fields for the macroscopic description	12
2.1.4	Domain theory	13
2.1.5	Stoner-Wohlfarth model	18
2.1.6	Magnetization reversal by curling	20
2.1.7	Micromagnetism	21
2.2	Domain walls in ferromagnetic nanowires	23
2.2.1	Preparation of domain walls	23
2.2.2	Depinning and motion of domain walls	27
2.3	Magnetoresistive effects	29
2.3.1	Spin-dependent transport	29
2.3.2	Lorentz magnetoresistance	31
2.3.3	Negative magnetoresistance	31
2.3.4	Anisotropic magnetoresistance	31
2.3.5	Domain-wall resistance	32
2.4	X-ray magnetic circular dichroism	33
3	Micromagnetic simulations	35
3.1	Method	35
3.2	Examples	39
3.2.1	Magnetic states of a tube	39
3.2.2	Demagnetization fields, nucleation, and reversal modes in cylindrical wires	40
4	Methods	45
4.1	Synthesis of cylindrical nanowires and sample preparation	45
4.2	Magnetoresistance measurements	48
4.3	Magnetic force microscopy	58
4.4	Photoemission electron microscopy	62



5 Magnetization reversal in cylindrical nickel nanowires	73
5.1 Magnetization reversal in straight nickel nanowires and the curling model	74
5.2 Experimental results	90
6 Preparation of domain walls in cylindrical nanowires	109
6.1 Ion irradiation	109
6.2 Bent wires	116
6.3 Diameter-modulated wires	120
7 Magnetization reversal in Co/Pt wires with perpendicular magnetic anisotropy	143
8 Conclusion	151
A Publications	155
A.1 Magnetic reversal of cylindrical nickel nanowires with modulated diameters	155
A.2 Domain-wall pinning and depinning at soft spots in magnetic nanowires	162
B Experimental details	167
B.1 Synthesis parameters for cylindrical wires	167
B.1.1 Nickel wires with one diameter modulation	167
B.1.2 Nickel-iron wires with one diameter modulation	168
B.1.3 Nickel wires with three modulations	168
B.2 Wafer substrates	169
B.3 Electron-beam lithography	170
B.3.1 Process parameters	170
B.3.2 Definition of contacts on self-arranged nanostructures	172
B.4 Optical projection lithography	174
B.5 Parameters for RF-plasma and sputter deposition	175
B.6 Transmission x-ray microscopy	176
B.6.1 Setup	176
B.6.2 Magnetic imaging of cylindrical nickel nanowires	177
B.7 Procedure for the elimination of thermal drift in Fig. 5.11(b)	178
B.8 Magnetization reversal in cobalt-nickel nanowires	179
Bibliography	181

1 Introduction

The performance of magnetic nanostructures is determined by their precisely engineered design and material properties. Therefore, their detailed inspection is indispensable prior to sensitive applications in many fields that range from local drug delivery or hyperthermia tumor treatment [Pan03] to high-density information storage [Ter05]. One focus of this work lies on establishing a novel x-ray method based on conventionally surface-sensitive photoemission electron microscopy that allows for the element-specific magnetic imaging of composite nanostructures as well as for the separate imaging of surface and bulk contributions [Kim11]. In particular in the field of magnetic data storage, industrial progress and underlying research have been exceptionally close ever since. Reaching fundamental limits such as superparamagnetism of down-scaled bits and unaddressability of non-perfect self-organized structures demands completely new concepts. In this respect, the so-called racetrack memory was proposed [Par05, Par08]. This non-volatile shift register is based on the effect that domain walls can be displaced by spin-polarized currents [Ber84, Klä03a, Tho07]. Franken *et al.* recently demonstrated a comparable concept based on field-driven domain-wall motion [Fra12c]. The precondition for the realization of such shift registers is to understand and control the pinning and the simultaneous propagation of domain walls in a periodic potential. Other promising applications basing on domain-wall motion are logic devices [All05] and lab-on-chip devices where micro-beads trapped in the stray-fields of domain walls are employed for the directed transportation of biomolecules and cells [Bry10, Rap12]. Systematic studies of field- and current-driven domain-wall dynamics are prerequisites for the realization of the above mentioned devices. These studies require the reliable preparation of domain walls. Since high current densities can change or destroy the structures investigated, weak pinning potentials allowing for the depinning of domain walls at low current densities are desirable. It is decisive for the preparation of a domain wall at such pinning sites, that the domain wall is injected into a wire at fields smaller than the field required to depin the domain wall from the respective pinning site.

The perspective of this work is to find reliable methods for the preparation of domain walls in two different kinds of ferromagnetic nanostructures, namely lithographically patterned wires of Co/Pt multilayers with perpendicular magnetic anisotropy and electrochemically synthesized nickel and nickel-iron wires. Both systems are among the most promising candidates for novel devices that are based on the propagation of domain walls. Furthermore, they can serve as model systems for fundamental studies.

Systems with high uniaxial out-of-plane anisotropy as Co/Pt multilayers are characterized by comparably small domain-wall widths. Thus, they allow for higher storage density compared to in-plane magnetized materials. It has been shown both theoretically [Tat04, Xia06] and experimentally [Bou08, Alv10] that the non-adiabatic spin transfer, an effect that increases with decreasing domain-wall width, contributes to the efficiency of current-driven domain-wall motion. Another advantage of systems with high perpendicular magnetic anisotropy is that one-dimensional models can be applied to analyze their domain walls, which exhibit nearly perfect Bloch or Néel spin structures [Bou11], whereas in soft-magnetic wires with a stray-field driven in-plane magnetization complex two-dimensional spin structures with intrinsic degrees of freedom occur [Hay06b]. The simple domain-wall structure is also the reason why for example Co/Pt layered structures with out-of-plane anisotropy are frequently used to investigate the intrinsic domain wall resistance [Has06, Azi06, Fra12b]. Furthermore, for Bloch walls in perpendicularly magnetized wires the domain-wall resistance is not masked by contributions of the anisotropic magnetoresistance as the magnetization is orthogonal to the current direction everywhere.

Anodization of aluminum templates allows for the creation of pores with modulated diameters [Lee06]. The pores can be covered by atomic-layer deposition or filled by electrochemical deposition to synthesize complex three-dimensional nanostructures replicating the variations of the pore diameter [Pit09, Cho10, Pit11]. The possibility of cheap mass production of uniform particles with diameters down to about 20 nm and aspect ratios up to 1000 makes this synthesis approach highly attractive for technological applications. It has been predicted that domain walls in cylindrical nanowires can act as massless objects [Yan10]. This implies that there is no Walker breakdown restricting the domain-wall velocity, and accordingly no fundamental limit for the performance of devices that are based on the fast movement of domain walls. Another aspect that is of interest for such applications is that there exists no threshold current for the displacement of massless domain walls. Soft-magnetic cylindrical wires are often declared as model systems for numerical simulations and analytical calculations based on infinite cylinders [Aha97a]. The validity of this approach is critically discussed in this work.

This thesis is structured as follows: chapter 2 gives an overview of the underlying physics. Section 2.1 focuses on the fundamentals of ferromagnetism including domain-wall theory. Section 2.2 deals with the preparation, depinning, and motion of domain walls in ferromagnetic nanowires. Introductions to magnetoresistive effects and to the x-ray magnetic circular dichroism (XMCD) effect, which is the basis of magnetic imaging using polarized x rays, follow in Secs. 2.3 and 2.4. Chapters 3 through 6 are dedicated to cylindrical nanowires. Chapter 3 gives an introduction to micromagnetic simulations and presents some results to illustrate the influence different energies have on the magnetic behavior of nanostructures. The synthesis of cylindrical nanowires as well as the methods employed for their characterization,

namely magnetoresistance measurements, magnetic force microscopy, and photoemission electron microscopy, are presented in chapter 4. Section 4.4 includes publication [Kim11] dealing with photoemission electron microscopy of three-dimensional magnetization configurations in core-shell nanostructures. Chapter 5 covers the results on straight nickel wires which are analyzed on the basis of the analytical curling model and micromagnetic simulations. The feasibility of controlled domain-wall preparation in wires manipulated with a focused ion beam, in bent wires, and in wires with diameter modulations serving as tailored pinning sites is the subject matter of chapter 6. Experimental aspects and results on Co/Pt multilayer wires are presented in chapter 7 that includes publication [Kim13]. Additional details on the sample preparation and magnetic imaging by transmission x-ray microscopy are given in the Appendix Secs. B.3 and B.6, respectively. The work closes with a conclusion in chapter 8.



Dieses Werk ist copyrightgeschützt und darf in keiner Form vervielfältigt werden noch an Dritte weitergegeben werden.
Es gilt nur für den persönlichen Gebrauch.

2 Fundamentals

In this work, magnetization reversal in two different kinds of ferromagnetic nanostructures, namely cylindrical nanowires and flat wires of Co/Pt multilayers, is studied. This chapter gives an overview of the underlying physics. The first section starts with the fundamentals of ferromagnetism and domain theory. Subsections 2.1.5 and 2.1.6 discuss the Stoner-Wohlfarth model of coherent rotation and the curling model, two models for the analytical treatment of magnetization reversal. The section closes with an introduction to micromagnetism, the basis for micromagnetic simulations. Section 2.2 deals with the preparation, depinning, and motion of domain walls in ferromagnetic nanowires. An introduction to spin-dependent transport and a phenomenological overview of magnetoresistive effects follows in Sec. 2.3. In Sec. 2.4 the x-ray magnetic circular dichroism (XMCD) effect, which is the basis of magnetic imaging using polarized x rays, is explained.

2.1 Ferromagnetism

Magnetism has been an active field of study for more than 2 500 years [Stö06]. Many theoretical and experimental approaches have generated a variety of definitions and concepts. Addressing all exciting aspects of the topic lies beyond the scope of this work. This section is limited to the basics and to the aspects directly related to this work: the microscopic origin of ferromagnetism, vector fields used for its description, as well as energy considerations and reversal modes regarding the formation of ferromagnetic patterns, so-called domains.

2.1.1 Origin of ferromagnetism

In a free atom, there are three origins of a magnetic moment: the spin of the electron, the orbital angular momentum of the electron with respect to the movement around the core, and changes of the orbital angular momentum induced by an external magnetic field [Spa11]. The latter leads to diamagnetism, while the other two aspects are the sources of paramagnetism. Some paramagnetic materials show a phase transition at the so-called Curie temperature. Below this temperature cooperative magnetic ordering appears, and the material is ferromagnetic. Classical magnetic dipole-dipole



interactions between adjacent ions are not strong enough to account for such a spontaneous magnetization, since ordering is easily destroyed by thermal fluctuations at temperatures above a few millikelvin [Kop07]. The orientation of the magnetic moments in a ferromagnet is a quantum-mechanical phenomenon [Blu01]. The basic interaction is the exchange interaction. The Hamiltonian considering the exchange energy between two fermionic particles with spins \vec{S}_i and \vec{S}_j is given by [Whi07]

$$\hat{H}_{\text{ex}} = -2J\vec{S}_i \cdot \vec{S}_j. \quad (2.1)$$

J is the coupling constant depending on the difference between the symmetric and the antisymmetric product state of the single-particle wavefunctions. This Hamiltonian is the basis of some fundamental models for the description of ferromagnetic behavior. The most popular of these models is the **Heisenberg model** where the interaction between the individual spins in a three-dimensional lattice is described by the Heisenberg Hamiltonian

$$\hat{H} = - \sum_{i \neq j} J_{ij} \vec{S}_i \cdot \vec{S}_j \quad (2.2)$$

with the exchange integral $J_{ij} = \int \int \psi_i(\vec{r}_1)\psi_j(\vec{r}_2) \frac{e^2}{4\pi\epsilon_0 r_{12}} \psi_i^*(\vec{r}_2)\psi_j^*(\vec{r}_1) d\vec{r}_1 d\vec{r}_2$ [Hei28]. ψ_{ij} are the single-particle wavefunctions, $\epsilon_0 \cong 8.854 \cdot 10^{-12} \frac{\text{As}}{\text{Vm}}$ is the permittivity of vacuum, and $e \cong 1.602 \cdot 10^{-19}$ C is the elementary charge.

If J is positive the system prefers parallel spin orientation and the material is ferromagnetic. For negative J antiparallel alignment is favored and the material shows an antiferromagnetic spin structure. Only in few materials the exchange interaction is strong enough to force an alignment of adjacent spins. If there is no overlap of the electron wave functions the Hamiltonian is zero and magnetic ordering cannot be explained by direct exchange interaction [Stö06]. Indirect exchange interaction can be mediated by a diamagnetic ion between two magnetic ions, e.g. manganese oxide, or via excited states, e.g. europium oxide [Mat61]. Another type of indirect exchange is the Ruderman-Kittel-Kasuya-Yoshida (RKKY) interaction [Rud54]. This long-range interaction is caused by the coupling of the magnetic moments of well-shielded, low lying shells to the conduction electrons. It shows an oscillatory behavior depending on the distance between two ions [Nol86]. The RKKY interaction is responsible for the coupling between magnetic layers, the basis of giant magnetoresistance (GMR).

In the 3d transition metals iron, cobalt, and nickel as well as in their alloys, the main exchange interaction is mediated by the conduction electrons. The origin of ferromagnetic order in such systems can be described by the **Stoner model of ferromagnetism**, which incorporates the exchange interaction into the itinerant electron model [Sto38]. The model considers the density of states $D(E)$ as consisting of two subbands $D_\uparrow(E)$ and $D_\downarrow(E)$ for electrons with spin up and spin down, respectively.

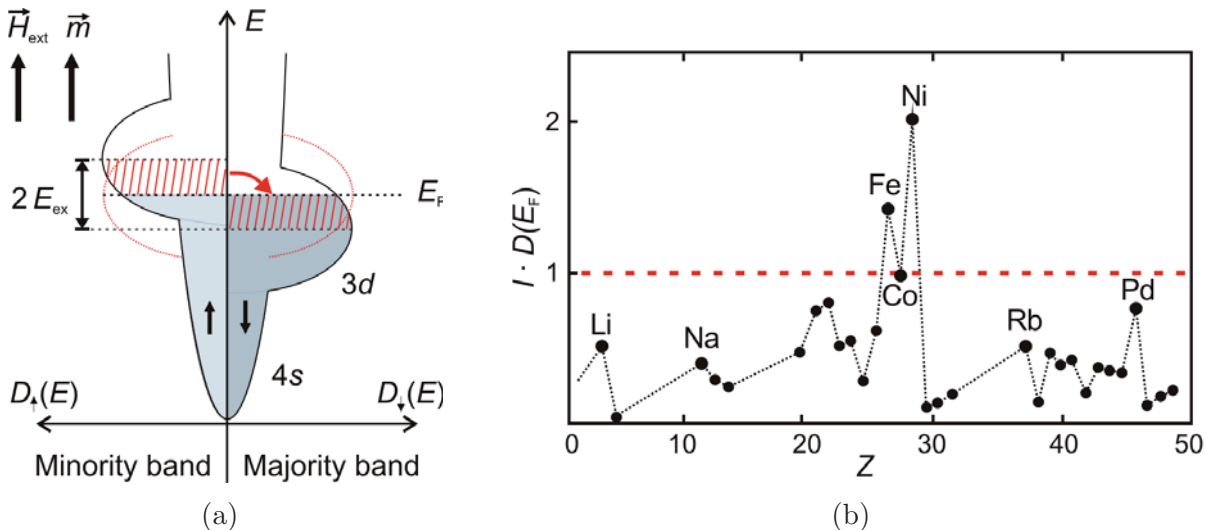


Figure 2.1: (a) Schematic of the spin-projected density of states of a 3d transition metal. Due to the exchange interaction the energy of the 3d electrons with a spin orientation antiparallel to the direction of an external field \vec{H}_{ext} is lower by the exchange splitting $2E_{\text{ex}}$ what leads to a population change as indicated by the red shaded regions. The gray areas mark the resulting filled electron states below the Fermi energy E_F . The band with the larger amount of electrons with spin down is called ‘majority band’, while the other one is referred to as ‘minority band’ carrying the minority electrons. (b) Product of the density of states at the Fermi level $D(E_F)$ and exchange integral I as a function of the atomic number Z . If the Stoner criterion $I \cdot D(E_F) \geq 1$ is fulfilled, a metal is ferromagnetic. After [Iba99].

In the presence of a magnetic field the degeneracy of electrons with opposite spin orientation is lifted and the two subbands get shifted by $\pm E_{\text{ex}}$. Electrons change from one subband to the other as indicated by the red shaded areas in Fig. 2.1(a). The increase in kinetic energy pays off by the energy reduction due to exchange interaction. The resulting difference in the number of electrons with spin up and spin down, also referred to as ‘minority’ and ‘majority’ electrons, leads to an effective magnetic moment \vec{m} . This magnetic moment is not necessarily an integer multiple of the Bohr magneton¹, as it is observed in iron ($2.2 \mu_B/\text{atom}$), cobalt ($1.7 \mu_B/\text{atom}$), and nickel ($0.6 \mu_B/\text{atom}$) [O'H00]. The model predicts a ferromagnetic ordering if the **Stoner criterion**

$$I \cdot D(E_F) \geq 1 \quad (2.3)$$

is fulfilled [Sto38]. I is an exchange integral, and $D(E_F)$ is the density of states at the Fermi level.

¹The Bohr magneton is defined as $\mu_B = \frac{e\hbar}{2m_e} \cong 9.27 \cdot 10^{-24} \text{ Am}^2$. $m_e \cong 9.109 \cdot 10^{-31} \text{ kg}$ is the electron mass, \hbar is Planck’s constant divided by 2π .

In Fig. 2.1(b) the product $D(E_F) \cdot I$ is plotted for some materials. The 3d transition metals iron (Fe), cobalt (Co), and nickel (Ni) are ferromagnetic as predicted by the Stoner criterion. While I is element specific and not depending on the local environment, $D(E_F)$ is influenced by adjacent ions. Atoms at interfaces have less neighbors, i.e. the coordination number is decreased. As a consequence the 3d band carrying the magnetic moment gets narrower and tends to the bandstructure of a free atom [Bob04]. The bandwidth is inversely proportional to the density of states at the Fermi level. That is why more metals satisfy the Stoner criterion if surface effects come into play. Palladium (Pd) and platinum (Pt) for example can be ferromagnetic if they are prepared as thin films [Blü95].

2.1.2 Magnetic anisotropy

Anisotropy means that a physical property is a function of direction. The spontaneous magnetization of a ferromagnet is not oriented arbitrarily but aligned along preferential directions, the so-called easy axes (EA). Without this anisotropy magnetic order could hardly be observed, especially in two dimensional systems such as thin films [Bla94]. The reason for this is the short-range character of the exchange interaction. Magnetic anisotropy is usually caused by different contributions made up of surface and volume parts. The individual contributions are discussed below.

Surface and interface anisotropy originate from missing neighbors. At interfaces the overlap of the electron shells is reduced. This modifies the exchange energy and results in an anisotropic magnetization behavior [Cho69].

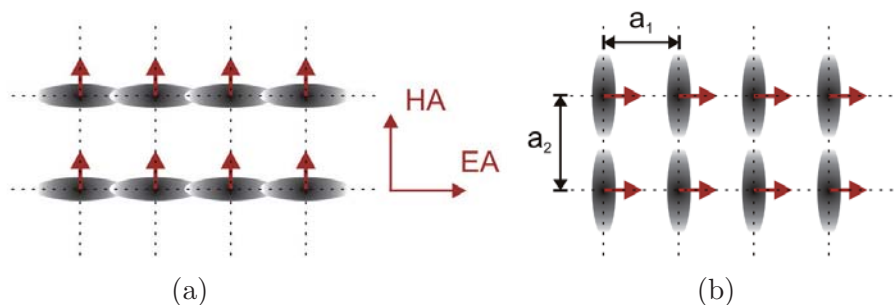


Figure 2.2: Microscopic origin of magnetocrystalline anisotropy. The gray shaded ellipses represent non-spherical charge distributions caused by spin-orbit interaction. In a cubic crystal with two different lattice constants a_1 and $a_2 > a_1$ the overlap of electron shells varies depending on the orientation of the associated magnetic moments indicated by the red arrows. For a hard axis (HA) magnetization the overlap is large (a), while for a magnetization along the easy axis (EA) the overlap and the concomitant exchange and electrostatic energy are reduced (b). After [Kit05].

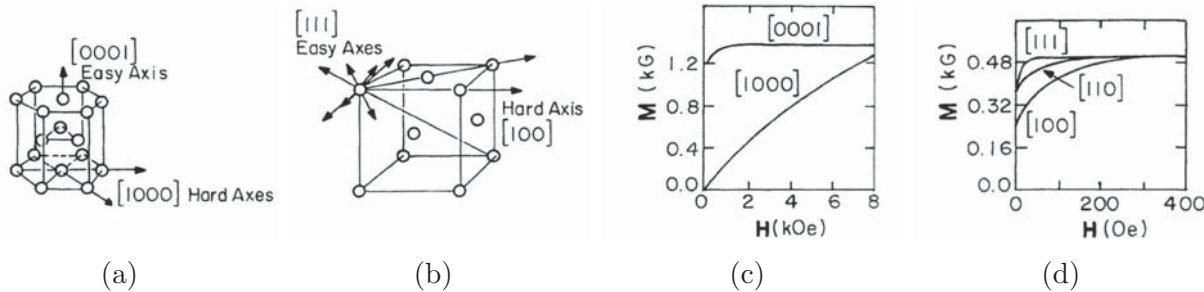


Figure 2.3: (a) Hexagonal lattice structure of cobalt. (b) Face-centered cubic (fcc) structure of nickel. Magnetization versus field curves of (c) cobalt and (d) nickel for an external magnetic field H applied along different crystal axes. Reprinted with permission from [O'H00]. Copyright 2000 by John Wiley and Sons.

The volume anisotropy has several origins. **Magnetocrystalline anisotropy** reflects the symmetry of the crystal lattice [Kit49]. Its microscopic origin is illustrated in Fig. 2.2. The electron distribution of an atom is coupled to the spin direction. It is not always spherical but can be deformed by spin-orbit interaction. If in addition the crystal field seen by an atom is of low symmetry, an anisotropic interaction of the electron shells with the crystal field can be observed. Phenomenologically the magnetocrystalline anisotropy is defined as the largest difference of spin-orbit energy for a sample magnetized along two different directions. For strong spin-orbit interaction and anisotropic crystal fields as they are typical for rare-earth metals, the magnetocrystalline anisotropy is high [Bré07]. If the coupling of the orbital angular momentum to the lattice is stronger than the spin-orbit coupling, a rather weak magnetocrystalline anisotropy is observed. The latter is generally the case in $3d$ transition metals. Nevertheless, magnetocrystalline anisotropy can play a role in these materials, and shall be discussed for cobalt and nickel in the following.

Figure 2.3 shows the crystal structures of cobalt and nickel as well as their magnetization versus field curves² along different crystal axes. The hexagonal crystal structure of cobalt results in a uniaxial magnetocrystalline anisotropy with an easy axis along the c axis ($\langle 0001 \rangle$ direction). As revealed by the magnetization curves in Fig. 2.3(c) high external fields are required to align the magnetic moments of cobalt parallel to the basal plane. The magnetic field required to saturate the magnetization of a sample along a hard axis is called anisotropy field H_a . It is a quantitative measure for the strength of the magnetocrystalline anisotropy.

In systems with one preferred direction as cobalt or thin films with uniaxial magnetic anisotropy, the anisotropy energy density is given by [Hub09]

$$\epsilon_{\text{uniaxial}} = K_{u1} \sin^2 \theta + K_{u2} \sin^4 \theta + \dots \quad (2.4)$$

²Magnetization curves are discussed in more detail in the respective paragraph of Sec. 2.1.4.